International Journal of Nanomedicine

Dovepress
Taylor & Francis Group

Open Access Full Text Article

ORIGINAL RESEARCH

T Cell-Derived Apoptotic Extracellular Vesicles Ameliorate Bone Loss via CD39 and CD73-Mediated ATP Hydrolysis

Xiaoshan Yang[1–3,*], Yang Zhou[2,3,*], Fuxing Zhou[4,*], Lili Bao[2,3], Zhengyan Wang[5], Zihan Li[2,3], Feng Ding[2,3], Huijuan Kuang[6,7], Huan Liu[8], Shenglong Tan[1], Xinyuan Qiu[1], Huan Jing[9], Shiyu Liu[2,3], Dandan Ma[1]

[1]Department of Endodontics, Stomatological Hospital, School of Stomatology, Southern Medical University, Guangzhou, 510280, People's Republic of China; [2]State Key Laboratory of Oral & Maxillofacial Reconstruction and Regeneration, National Clinical Research Center for Oral Diseases, Shaanxi Key Laboratory of Stomatology, Department of Oral Biology, School of Stomatology, The Fourth Military Medical University, Xi'an, 710032, People's Republic of China; [3]State Key Laboratory of Oral & Maxillofacial Reconstruction and Regeneration, National Clinical Research Center for Oral Diseases, Shaanxi International Joint Research Center for Oral Diseases, Center for Tissue Engineering, School of Stomatology, The Fourth Military Medical University, Xi'an, 710032, People's Republic of China; [4]Department of Gynecology and Obstetrics, Xijing Hospital, The Fourth Military Medical University, Xi'an, 710032, People's Republic of China; [5]Department of Orthodontics, School and Hospital of Stomatology, Cheeloo College of Medicine, Shandong University & Shandong Key Laboratory of Oral Tissue Regeneration & Shandong Engineering Research Center of Dental Materials and Oral Tissue Regeneration & Shandong Provincial Clinical Research Center for Oral Diseases, Jinan, 250012, People's Republic of China; [6]Department of Orthopaedics, The First Affiliated Hospital of Xi'an Jiaotong University, Xi'an, 710061, People's Republic of China; [7]State Key Laboratory for Manufacturing System Engineering, Xi'an Jiaotong University, Xi'an, 710054, People's Republic of China; [8]Department of Otolaryngology Head and Neck Surgery, Peking University Third Hospital, Beijing, 100871, People's Republic of China; [9]Department of Endodontics, Guangdong Provincial High-level Clinical Key Specialty, Guangdong Province Engineering Research Center of Oral Disease Diagnosis and Treatment, Peking University Shenzhen Hospital, Shenzhen, 518036, People's Republic of China

*These authors contributed equally to this work

Correspondence: Dandan Ma, Stomatological Hospital, Southern Medical University, S366 Jiangnan Boulevard, Guangzhou, Guangdong, 510280, People's Republic of China, Tel +86-20-34152996, Email mdd@smu.edu.cn; Shiyu Liu, School of Stomatology, The Fourth Military Medical University, No. 145, West Changle Road, Xi'an, Shaanxi, 710032, People's Republic of China, Tel +86-29-84772645, Email liushiyu@vip.163.com

Background: Osteoporosis is a major public health concern characterized by decreased bone density. Among various therapeutic strategies, apoptotic extracellular vesicles (ApoEVs) have emerged as promising agents in tissue regeneration. Specifically, T cell-derived ApoEVs have shown substantial potential in facilitating bone regeneration. However, it remains unclear whether ApoEVs can promote bone mass recovery through enzymatic activity mediated by membrane surface molecules. Therefore, this study aimed to investigate whether T cell-derived ApoEVs could promote bone mass recovery in osteoporosis mice and reveal the underlying mechanisms.

Methods: ApoEVs were isolated through sequential centrifugation, and their proteomic profiles were identified via mass spectrometry. Western blot and immunogold staining confirmed the enrichment of CD39 and CD73 on ApoEVs. The role of CD39 and CD73 in hydrolyzing adenosine triphosphate (ATP) to adenosine was evaluated by quantifying the levels of ATP and adenosine. Inhibitors of CD39 and CD73, and an A2BR antagonist were used to explore the molecular mechanism of ApoEVs in promoting bone regeneration.

Results: ApoEVs significantly reduced bone loss and promote the osteogenic differentiation of BMMSCs in ovariectomy (OVX) mice. We observed increased levels of extracellular ATP and a decrease in CD39 and CD73, key enzymes in ATP-to-adenosine conversion in bone marrow of OVX mice. We found that ApoEVs are enriched with CD39 and CD73 on their membranes, which enable the hydrolysis of extracellular ATP to adenosine both in vitro and in vivo. The adenosine generated by ApoEVs inhibits the inflammatory response and promotes osteogenesis through A2BR and downstream PKA signaling.

Conclusion: T cell-derived ApoEVs are enriched with CD39 and CD73, enabling them to hydrolyze extracellular ATP to adenosine, thereby promoting bone regeneration via A2BR and PKA signaling pathway. Our data underscore the substantive role of T cell-derived ApoEVs to treat osteoporosis, thus providing new ideas for the development of ApoEVs-based therapies in tissue regeneration.

Keywords: T cell apoptosis, apoptotic extracellular vesicles, CD39, CD73, adenosine, bone regeneration

Received: 13 August 2024
Accepted: 20 January 2025
Published: 27 January 2025

Graphical Abstract

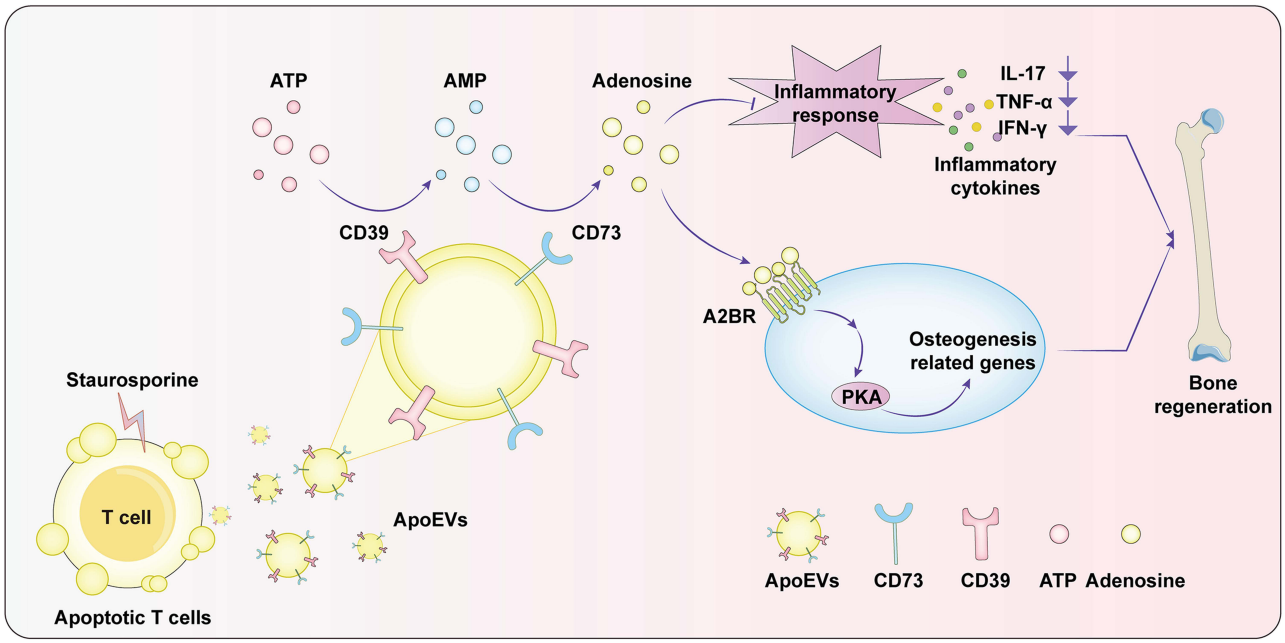

Introduction

Osteoporosis is a disease characterized by decreased bone mass and deterioration of bone micro-architecture, often affecting postmenopausal women due to estrogen deficiency.[1] Current therapeutic agents for osteoporosis treatment have shown limited efficacy and adverse side effects.[2,3] Bisphosphonates are the most widely used drugs for osteoporosis, the main concerns limiting their use including atypical femur fractures and osteonecrosis of the jaw.[2–4] While estrogen therapy has proven effective in preventing and treating osteoporosis, its associated risks, such as an increased incidence of cardiovascular events and the potential to raise the risk of breast cancer, limit its suitability as a long-term treatment for osteoporosis.[5] Therefore, there is an urgent need for safe and effective therapeutic interventions.

Studies have shown that activated T cells are key mediators of ovariectomy (OVX)-induced bone loss since they contribute to elevated levels of proinflammatory cytokines and promote osteoclast differentiation.[6,7] It has been established that lymphocyte apoptosis plays an important role in regulating inflammation and maintaining physiological homeostasis.[8,9] Previous research from our group demonstrated that inducing apoptosis in activated T cell in vivo restores immune homeostasis and promotes bone mass recovery in osteoporotic mice.[10] However, the underlying molecular mechanisms remain to be elucidated. During apoptosis, cells release a large number of apoptotic extracellular vesicles (ApoEVs) that show a great potential in modulating immune response and facilitating tissue repair.[11–14] Recent studies have demonstrated that ApoEVs can significantly enhance dental pulp regeneration by activating autophagy.[15] Moreover, ApoEVs can target hepatic macrophages, modulating their migration, polarization, and functionality.[11] Alternatively, ApoEVs have been found to promote wound healing and hair growth in skin and hair follicle mesenchymal stem cells.[16] As for ApoEVs released by T cells, the natural membrane of these ApoEVs grants them the capability to target inflammatory regions and regulate inflammatory processes.[17] Furthermore, engineered chimeric T cell-derived ApoEVs, functionalized with natural membrane and modular delivery system, can effectively modulate inflammation and ameliorate the inflammatory bowel disease.[18] Collectively, these findings confirm that T cell-derived ApoEVs possess the capability to regulate the immune response and facilitate tissue repair, highlighting their potential therapeutic applications in osteoporosis. Current understanding of extracellular vesicles mainly focusses on their role as carriers of biomolecular content and therapeutic agents. Despite their small size, ApoEVs provide a substantial amount of

membrane surface area.[19,20] However, there is still a limited amount of research on how ApoEVs utilize their surface molecules to exert their functions.

CD39 (ectonucleoside triphosphate diphosphohydrolase-1) and CD73 (ecto-5′-nucleotidase) are membrane-bound ectonucleotidases that regulate extracellular adenosine triphosphate (ATP) and adenosine by hydrolyzing extracellular ATP to adenosine monophosphate (AMP) and AMP to adenosine, respectively.[21,22] Extracellular ATP is a danger signal and functions as an immunostimulatory signal. By activating cell surface receptors, ATP triggers pro-inflammatory immune responses. Conversely, adenosine possesses potent anti-inflammatory properties and suppresses immune responses.[23] Therefore, CD39 and CD73 facilitate the transition from a pro-inflammatory to an anti-inflammatory environment by hydrolyzing ATP to adenosine.[21] More importantly, the interconversion between ATP and adenosine is pivotal in maintaining bone homeostasis. ATP has been shown to promote osteoclast differentiation and induce bone resorption,[24] while adenosine can promote the proliferation of mouse bone marrow mesenchymal stem cells (BMMSCs), and positively modulate the vitality of osteoblasts.[25,26] Consequently, CD39 and CD73, as key extracellular enzymes in the ATP-to-adenosine hydrolysis pathway, are potential targets for modulating bone homeostasis. However, it remains unclear whether T cell-derived ApoEVs express CD39 and CD73 on their surface and promote bone formation through the enzymatic activity of these ectonucleotidases. We hereby hypothesize that T cell-derived ApoEVs, through the action of CD39 and CD73, promote bone regeneration by converting extracellular ATP to adenosine.

In the present study, we isolated T cell-derived ApoEVs and found that ApoEVs mitigate osteopenia and rescues the osteogenic deficiency of BMMSCs in OVX mice. Notably, this effect was not observed with apoptotic T cells (ApoEVs-free). We characterized the proteomic profiles of ApoEVs and apoptotic T cells, and identified a distinct enrichment of certain ectonucleotidases on the surface of ApoEVs compared with apoptotic T cells. Subsequent investigations revealed elevated levels of extracellular ATP in the bone marrow of OVX mice, accompanied with reduced expression of CD39 and CD73. Importantly, we demonstrated that ApoEVs were enriched with CD39 and CD73 on their membrane surface, enabling them to hydrolyze extracellular ATP to adenosine. This enzymatic activity regulated the immune microenvironment and facilitated osteogenic differentiation by activating the A2B adenosine receptor (A2BR) and downstream protein kinase A (PKA) signaling pathway. Taken together, these findings extended our understanding of ApoEVs, unravelling their capacity to hydrolyze extracellular ATP and their potential in promoting bone regeneration.

Materials and Methods

Mice

Female C57BL/6 mice housed under a 12-h light/12-h dark cycle, with food and water given ad libitum. All animal procedures were approved by the Institutional Animal Care and Use Committee at Southern Medical University and followed all aspects of Guidelines for the Care and Use of Laboratory Animals.

Isolation and Activation of Splenic Pan T Cells

Mouse spleens were crushed and filtered to form a single-cell suspension. ACK lysis buffer (Beyotime, C3702) was used to remove red blood cells. The cell suspension was cultured in RPMI 1640 medium (Gibco) supplemented with 10% fetal bovine serum (FBS), 50 mm 2-mercaptoethanol, 2 mm L-glutamine (Sigma-Aldrich), and 1% penicillin/streptomycin (Invitrogen). For T cell activation, the plate was coated with anti-CD3ε antibody (5 μg/mL in PBS) (BioLegend, 100340) for 4 hours at 37 °C prior to cell seeding. Cells were then cultured in RPMI 1640 medium with anti-CD28 antibody (2 μg/mL) (eBioscience, 16–0281-85). After 48 hours of incubation, T cells were activated.

Isolation of Apoptotic Extracellular Vesicles (ApoEVs)

Activated T cells were treated with staurosporine (Cell Signaling Technology, 9953) for 12 hours to induce apoptosis. ApoEVs were isolated from medium of apoptotic cells using a sequential centrifugation method as previously reported.[27] First, the culture media and cells were collected and subjected to centrifugation at 800 g for 10 minutes to pellet the cells and debris. The supernatant was then carefully transferred to a new tube and further centrifuged at 16000 g for 30 min at 4°C to concentrate the ApoEVs. After this step, the supernatant was removed, and the pellet was

washed twice with PBS. The purification process was completed by centrifuging the washed pellet at 16000 g for an additional 30 minutes at 4°C. Finally, the purified ApoEVs derived from T cells were resuspended in PBS and were ready for subsequent experiments. The concentration of ApoEVs was determined using a BCA protein assay kit (TIANGEN, PA115).

Characterization and Identification of ApoEVs

The morphology of ApoEVs was observed by scanning electron microscope (SEM) (Hitachi) and transmission electron microscope (TEM) (TECNAI Spirit, FEI). For size distribution evaluation, ApoEVs were diluted with PBS. The size of ApoEVs was examined using nanoparticle tracking analysis (NTA) with Zeta View (Particle Metrix) and corresponding software Zeta View. For apoptotic marker detection, ApoEVs were characterized by Western blot using anti-CD3, anti-Caspase-3 and anti-β-Tubulin antibodies, as stated below. Additionally, for phosphatidylserine (PtdSer) detection, ApoEVs were stained with PE-Annexin V (BD Biosciences Pharmingen, 559763) in binding buffer followed by observation under a confocal microscope (Nikon) and detection via a flow cytometer (Beckman), ApoEVs were defined as Annexin V-positive events.

Protein Isolation and Western Blot Analysis

Whole lysates of cells or ApoEVs were extracted using RIPA buffer (Beyotime, P0013B) supplemented with protease and phosphatase inhibitors (Sigma-Aldrich, S8830), while the membrane proteins were extracted by Membrane Protein Extraction Kit (Thermo Scientific, 89842) following the manufacturer's protocol. Equal amounts of protein samples were loaded onto sodium dodecyl sulfate-polyacrylamide gel electrophoresis (SDS-PAGE) and transferred to polyvinylidene fluoride (PVDF) membranes (Millipore). The membranes were blocked with 5% non-fat milk for 2 h at room temperature, followed by incubation overnight at 4°C with the following primary antibodies: anti-CD3 (Santa Cruz Biotechnology, sc-20047), anti-Caspase-3 (Cell Signaling Technology, 9662), anti-ALP (Abmart, T55421S), anti-Runx2 (Bimake, A5193), anti-CD39 (Abcam, ab227840), anti-CD73 (Abcam, ab288154), anti-A2BR (Abmart, PA3755S), anti-p-PKA (Cell Signaling Technology, 5661), anti-β-Tubulin (CWBIO, CW0098), and anti-GAPDH (CWBIO, CW0100). After washing with PBST (PBS containing 0.1% Tween 20), the membranes were incubated with secondary antibodies for 2 hours at room temperature. The protein bands were visualized with a Western-Light Chemiluminescent Detection System (Tanon). Quantification of digital images was performed using ImageJ software.

Establishment of Mice Osteoporosis and Treatment

Eight-week-old female C57BL/6 mice were anesthetized and subjected to either a sham operation (Sham) or bilateral ovariectomized (OVX). Briefly, mice were anesthetized with an intraperitoneal injection of sodium pentobarbital. The skin around the midline of the back was then shaved and disinfected. Linear incisions were made bilaterally on the skin along the lumbar vertebrae to expose ovaries. Then, the bilateral ovaries and fat tissues were gently removed from mice to establish the osteoporosis model, while the mice in the Sham group only had some adipose tissue around the ovary removed. Finally, the tissues were repositioned, and the fascia and skin wound were sutured carefully. Animals were monitored daily for general health and well-being to ensure the animals maintained a healthy state for the duration of the surgery. Four weeks later, femurs of mice were isolated after euthanasia for micro-CT scanning to confirm estrogen deficiency-induced osteoporosis.

For the treatment of OVX mice, mice were randomly separated into several groups using a computer-generated randomization list. PBS (150 μL), ApoEVs (100 μg in 150 μL PBS), apoptotic T cells (100 μg in 150 μL PBS), POM-1 (POM, CD39 inhibitor) pretreated ApoEVs (100 μg in 150 μL PBS), or PSB-12379 (PSB, CD73 inhibitor) pretreated ApoEVs (100 μg in 150 μL PBS) were infused intravenously through the tail vein once a week. For POM-1 or PSB-12379 pretreated ApoEVs groups, ApoEVs were preincubated with 100 μM POM-1 or 100 μM PSB-12379 for 40 min at room temperature. Four weeks after the treatment, mice were sacrificed for further analysis. Micro-computed tomography (Micro-CT) analysis was used to confirm the establishment of mice osteoporosis and evaluate therapeutic effects.

Micro-CT Analysis

Femora dissected from mice were fixed in 4% paraformaldehyde overnight and analyzed by high-resolution micro-CT (Bruker, SkyScan). The specimens were scanned using a voxel size of 8 μm at 55 kV and 200 μA. The image reconstruction software (NRecon), data analysis software (CTAn), and 3D model visualization software (μCTVol) were applied to analyze the scanned data. Bone mineral density (BMD, mg/cm^3), bone volume to tissue volume (BV/TV), trabecular number (Tb. N, 1/mm), and trabecular separation (Tb. Sp, mm) for each specimen were quantitatively analyzed.

In Vivo Biodistribution of ApoEVs in Tibiae and Femurs

To detect the distribution of ApoEVs in tibia and femur, ApoEVs were prelabeled with DiR (Yeasen Biotechnology, 40757ES25) according to the manufacturer's instructions, and injected intravenously into OVX mice. PBS was used as negative control. After 6, 12, 24, 36 and 48 hours, freshly dissected tibiae and femurs were collected and analyzed for the fluorescence signal. The luminescence was acquired for a few seconds in an ex vivo IVIS imaging system (PerkinElmer).

Isolation and Culture of Mouse Bone Marrow Mesenchymal Stem Cells (BMMSCs)

BMMSCs were flushed out of the tibiae and femurs from C57BL/6 mice. Briefly, tibiae and femurs were dissected out and cleaned of connective tissue. Bone marrow cells were flushed out from long bones by a syringe with α-MEM medium supplemented with 20% FBS, 2 mm L-glutamine (Sigma-Aldrich), and 1% penicillin/streptomycin (Invitrogen). Single-cell suspensions were seeded in dishes and initially maintained in an atmosphere of 5% CO_2 at 37 °C.

Osteogenic Differentiation Assay

For osteogenic differentiation, BMMSCs were seeded in 6-well (2×10^5 cells per well) or 12-well (1×10^5 cells per well) in α-MEM medium supplemented with 20% FBS, 2 mM L-glutamine (Sigma-Aldrich), and 1% penicillin/streptomycin (Invitrogen). When cells reached 80–90% confluence, the growth medium was changed into osteogenic differentiation medium: α-MEM with 10% FBS, 1% penicillin/streptomycin, 5 mM β-glycerophosphate, 50 μg/mL ascorbic acid and 10 nM dexamethasone (Sigma-Aldrich). The medium was refreshed every other day. For quantitative real-time PCR analysis, the cells underwent differentiation for 5 days in osteogenic differentiation medium. For Western blot assays, the differentiation period was extended to 10 days. Additionally, for alizarin red staining,[28] the cells were differentiated for 21 days, and the alizarin red staining was performed according to the manufacturer's instructions (Beyotime, C0148S). Photographs were taken by an inverted optical microscope. The quantitative analysis was conducted by dissolution with 10% cetylpyridinium chloride, and the OD value at 562 nm was measured.

RNA Extraction and Quantitative Real-Time PCR

Total RNA was extracted using TRIzol Reagent (Mishu Shengwu, MI00617) and cDNA was synthesized from 1 μg of total RNA by using the Reverse Transcription Kit (TaKaRa, RR037A). Next, real-time PCR was performed using a Quantitative SYBR Green Kit (Takara, RR820B) and detected by CFX 96Touch (Bio-Rad). Relative gene expression was calculated by the $-2\Delta\Delta Ct$ method and GAPDH was used as reference for normalization. Primer sequences used are listed below: ALP (Forward: 5′-CCAACTCTTTTGTGCCAGAGA-3′; Reverse: 5′-GGCTACATTGGTGTTGAGCTTTT-3′); Runx2 (Forward: 5′-GACTGTGGTTACCGTCATGGC-3′; Reverse: 5′-ACTTGGTTTTTCATAACAGCGGA-3′); A1R (Forward: 5′-CTACCTTCTGCTTCATCGTATC-3′; Reverse: 5′- GTACCGATCCACAGCAATAG-3′); A2AR (Forward: 5′-CCAACTTCTTCGTGGTATCTC-3′; Reverse: 5′- TCGGATGGCGATGTATCT-3′); A2BR (Forward: 5′-GCTCCATCTTTAGCCTCTTG-3′; Reverse: 5′-CTGGTGGCACTGTCTTTAC-3′); A3R (Forward: 5′-CTGCATCCTCCAGGTTAATG-3′; Reverse: 5′- GTCACAACAGTCCAGAGAAC-3′); GAPDH (Forward: 5′-TGTGTCCGTCGTGGATCTGA-3′; Reverse: 5′-TTGCTGTTGAAGTCGCAGGAG-3′).

Proteomic Analyses

Protein lysates of apoptotic T cells and ApoEVs were prepared. After rapid freezing in liquid nitrogen, samples were transported to Lc-Bio Technologies for subsequent analysis. Four-dimensional (4D) label-free quantitative proteomics analysis by time-of-flight mass spectrometry (Thermo Scientific) was performed to measure the protein content The reproducibility of the quantification results was assessed and evaluated, and the differentially expressed proteins were identified and subjected to functional classification and analysis. Proteins that were significantly upregulated in ApoEVs were included for further functional analysis based on Gene Ontology (GO) and Kyoto Encyclopedia of Genes and Genomes (KEGG) databases.

The Enzymatic Activity of ApoEVs in Hydrolyzing Adenosine Triphosphate (ATP)

To detect the enzymatic activity of ApoEVs and apoptotic T cells in hydrolyzing ATP, we established an in vitro reaction system. Firstly, 10 μM ATP was added into each well of a 96-well plate. Based on the experimental design, 0, 10, 20 or 30 μg/mL ApoEVs or apoptotic T cells and POM-1 (POM, a CD39 inhibitor) or PSB-12379 (PSB, a CD73 inhibitor) preincubated ApoEVs were added to the respective wells. To prepare CD39- or CD73-inhibited ApoEVs, 30 μg/mL of ApoEVs were preincubated with 100 μM POM (dissolved in DMSO, MedChemExpress) or PSB (dissolved in water, MedChemExpress) for 40 minutes at room temperature. The plate was then incubated in the dark for 30–45 min at room temperature. ATP concentration was determined as described below.

ATP and Adenosine Assay

Quantification of ATP was carried out using an enhanced ATP Assay Kit (Beyotime, S0027) following the manufacturer's protocol. For the detection of extracellular ATP levels in bone marrow, tibia and femur were flushed with 600 μL PBS to collect whole marrow. The flush was then centrifuged at 4000 rpm for 10 min at 4°C to separate the cell and plasma fractions. Samples and standard solutions (20 μL) were added to the 96-well plates containing the ATP reaction mix and incubated at room temperature in the dark for 1 min. The plates were read using a luminometer (PerkinElmer), and the ATP amount was calculated from the standard curve.

For the detection of adenosine, an adenosine assay kit (Abmart, AB-6078A) was used to measure the concentration of adenosine in plasma of bone marrow flush or the in vitro reaction system, according to the manufacturer's instructions.

Detection of CD39 and CD73 in Bone Marrow

The whole bone marrow flush was collected from tibia and femur as described above. The flush was centrifuged at 4000 rpm for 10 min at 4°C. Remove the supernatant and resuspend the pellet in RIPA buffer to lysis the proteins in bone marrow and obtain protein samples for subsequent experiments. Subsequently, Western blot was used to detect the expression of CD39 and CD73 in bone marrow from OVX mice and sham-operated mice.

Detection of CD39 and CD73 on the Surface of ApoEVs

To confirm the presence of CD39 and CD73 on the surface membrane of ApoEVs, Western blot and immunogold staining were conducted. For Western blot, membrane proteins of cells and ApoEVs were extracted as stated above. For immunogold staining, ApoEVs were mixed with an equal volume of 2.5% glutaraldehyde for 20 min at room temperature and then applied to 200-mesh nickel grids. After blocking with 5% BSA, the grid was incubated with a 1:50 dilution of the primary antibodies (anti-CD39 antibody and anti-CD73 antibody) overnight at 4 °C. After washing with ultrapure water, the grid was treated with 10-nm gold-labeled secondary antibody (Abcam, ab270555) for 30 min. The grid was then washed with ultrapure water and stained with 2% phosphotungstic acid hydrate for 30s, followed by rinsing with ultrapure water. After dying, all grids were examined by TEM (TECNAI Spirit, FEI).

Enzyme-Linked Immunosorbent Assays of Cytokines

Peripheral blood samples were collected from mice and centrifuged at 2500 rpm for 10 min to isolate serum. Mouse IFN-γ, IL-17, and TNF-α were detected using an ELISA kit (4abio) according to manufacturer's instructions.

Statistical Analysis

For multiple group comparisons, statistical significance was calculated by one-way ANOVA with Tukey's post hoc test. For two group comparisons, significance was assessed by unpaired Student's *t* test (two-tailed). All data were expressed as mean ± standard deviation (SD). GraphPad Prism 9 were used to analyze and visualize the data. P values less than 0.05 were considered significant.

Results

Isolation and Characterization of T Cell-Derived ApoEVs

We first investigated the biological properties of T cell-derived AopEVs. Splenic T cells were isolated and activated in vitro. Activated T cells showed larger size (Figure S1A) and higher expression of CD25 (Figure S1B) than those of unactivated T cells. Staurosporine (STS) was then used to induce apoptosis of activated T cells.[17] Subsequently, we isolated ApoEVs from apoptotic T cells using the optimized gradient centrifugation protocol (Figure 1A). The concentration of ApoEVs isolated from apoptotic T cells was significantly higher than that from activated T cells (Figure 1B). Subsequent analyses via scanning electron microscopy (SEM) and transmission electron microscopy (TEM) revealed

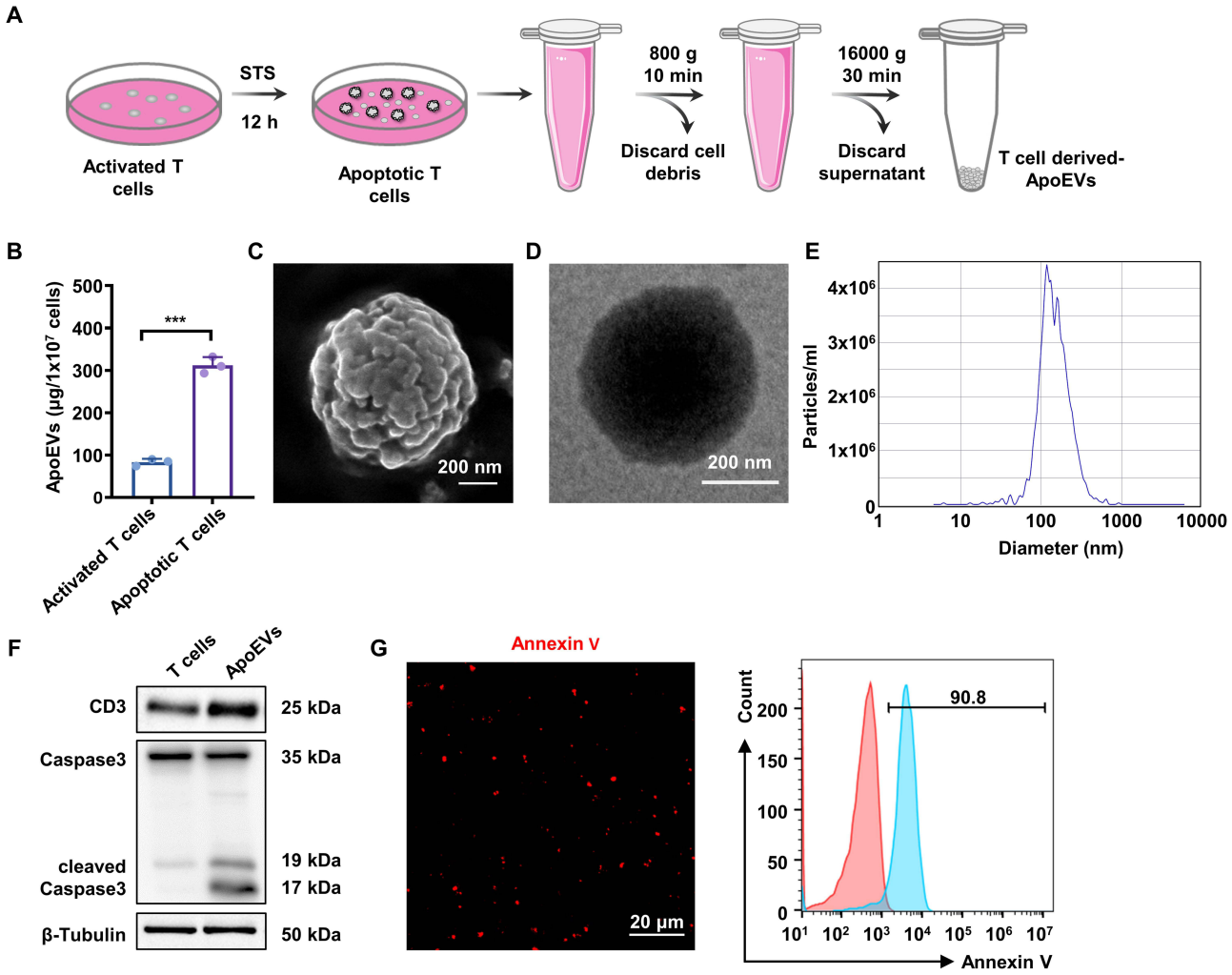

Figure 1 Isolation and characterization of T cell-derived ApoEVs. (**A**). The schematic diagram shows the isolation protocol of T cell-derived ApoEVs. (**B**). Quantification of T cell-derived ApoEVs after activated T cells were treated with STS for 12 hours (N = 3). (**C**). Representative scanning electron microscopy (SEM) image of T cell-derived ApoEVs (scale bar = 200 nm). (**D**). Representative transmission electron microscopy (TEM) image of T cell-derived ApoEVs (scale bar = 200 nm). (**E**) Size distribution of ApoEVs detected by nanoparticle tracking analysis (NTA). (**F**) Western blot analysis showing the presence of CD3 and Caspase-3/cleaved Caspase-3 in T cells and ApoEVs. (**G**) Representative confocal microscopy images (red) and flow cytometric analysis of Annexin V staining in ApoEVs (scale bar = 20 μm). Data are presented by mean ± SD; ***P< 0.001 by unpaired Student's *t* test.

https://doi.org/10.2147/IJN.S491222

a typical circular or elliptical morphology of ApoEVs (Figure 1C and D). Nanoparticle tracking analysis (NTA) showed that most ApoEVs were within the 100–600 nm diameter range (Figure 1E). Next, we detected the expression of membrane markers by Western blot. The results confirmed that ApoEVs expressed the same membrane marker, CD3, as T cells (Figure 1F). Additionally, the presence of cleaved Caspase-3, a specific marker of apoptotic cells, within ApoEVs was detected, suggesting the retention of apoptotic components in ApoEVs (Figure 1F). Immunofluorescent staining and flow cytometric analysis showed that ApoEVs were also positive for apoptosis-specific markers phosphatidylserine (PtdSer), as indicated by Annexin V staining (Figure 1G). These results indicated the successful induction of apoptosis in activated T cells and confirmed the specific characteristics of ApoEVs.

Systemic Infusion of ApoEVs Ameliorates Osteopenia and Rescues the Osteogenic Deficiency of BMMSCs in OVX Mice

ApoEVs have been shown to promote tissue development and regeneration in multiple systems.[17,29,30] In this study, we investigate whether T cell-derived ApoEVs could promote bone mass recovery in osteoporosis mice and reveal the underlying mechanism. Four weeks post-OVX surgery, femur bone mass was significantly reduced in OVX mice versus sham controls (Figure S2A). This was accompanied by decreased bone mineral density (BMD), bone volume to tissue volume (BV/TV), and trabecular number (Tb.N), as well as increased trabecular separation (Tb.Sp) in OVX mice (Figure S2B-E). These findings confirm the successful establishment of an osteoporosis model. The distribution of ApoEVs in tibiae and femurs was tested ex vivo. DiR-labeled ApoEVs were intravenously injected into the OVX mice and bone samples were collected for analysis at different time points (Figure 2A). Ex vivo fluorescence imaging revealed that ApoEVs distributed in tibiae and femurs approximately at 6 hours post-injection and then reached a peak at 24 hours (Figure 2A). Subsequently, OVX mice were infused intravenously with PBS or ApoEVs once a week for four weeks. Another one week later, bone mass of the femur was evaluated, with sham-operated mice serving as controls (Figure 2B). Micro-CT scanning revealed that ApoEVs significantly mitigated bone loss in OVX mice compared with the PBS group (Figure 2C), which was also emphasized by the quantities of BMD, BV/TV, Tb. N, and Tb. Sp (Figure 2D–G). To further illustrate the differentiation potential of BMMSCs, we cultured BMMSCs isolated from Sham mice, PBS- or ApoEVs-treated OVX mice in osteogenic differentiation medium. The results unveiled a remarkable increase in the osteogenic markers alkaline phosphatase (ALP) and runt-related transcription factor 2 (Runx2) at both mRNA and protein levels in OVX mice treated with ApoEVs compared to the PBS group (Figure 2H and I). Additionally, alizarin red staining (Figure 2J) of the calcium nodules was performed, and a similar conclusion could be drawn that the osteogenic differentiation ability of ApoEVs-treated OVX mice was significantly stronger than that of the PBS-treated OVX mice (Figure 2J). These results indicated that ApoEVs ameliorates osteopenia and enhances the osteogenic differentiation ability of BMMSCs in OVX mice.

Moreover, to verify the crucial role of ApoEVs secretion in promoting bone regeneration during apoptosis, we investigated whether the residual apoptotic T cell (ApoEVs-free) also have the potential to promote bone formation in OVX mice and compared their efficacy with that of ApoEVs. OVX mice received intravenous infusions of either ApoEVs or apoptotic T cells (ApoEVs-free) once a week for four weeks. Surprisingly, our findings revealed that apoptotic T cells failed to mitigate bone loss compared to the ApoEVs group (Figure S3A), which was also emphasized by the assessments of BMD, BV/TV, Tb. N, and Tb. Sp (Figure S3B-E). Collectively, these data indicated that ApoEVs, but not apoptotic T cells, ameliorate osteopenia and rescues the osteogenic deficiency of BMMSCs in OVX mice.

T Cell-Derived ApoEVs are Enriched With Specific Ectonucleotidases

To explore why ApoEVs was able to ameliorate osteopenia, the specific proteomic features of T cell-derived ApoEVs were identified. We prepared proteins samples of ApoEVs and parental apoptotic T cells (ApoEVs-free), and performed mass spectrometry analysis. A total of 6040 proteins were identified in ApoEVs and apoptotic T cells. Among the 680 differentially expressed proteins between the ApoEVs and apoptotic T cells, 215 were significantly upregulated in the ApoEVs (Figure 3A). To better understanding the upregulated proteins in ApoEVs, subcellular localization, Gene Ontology (GO) annotations and a Kyoto Encyclopedia of Genes and Genomes (KEGG) pathway analysis were performed (Figure 3B-

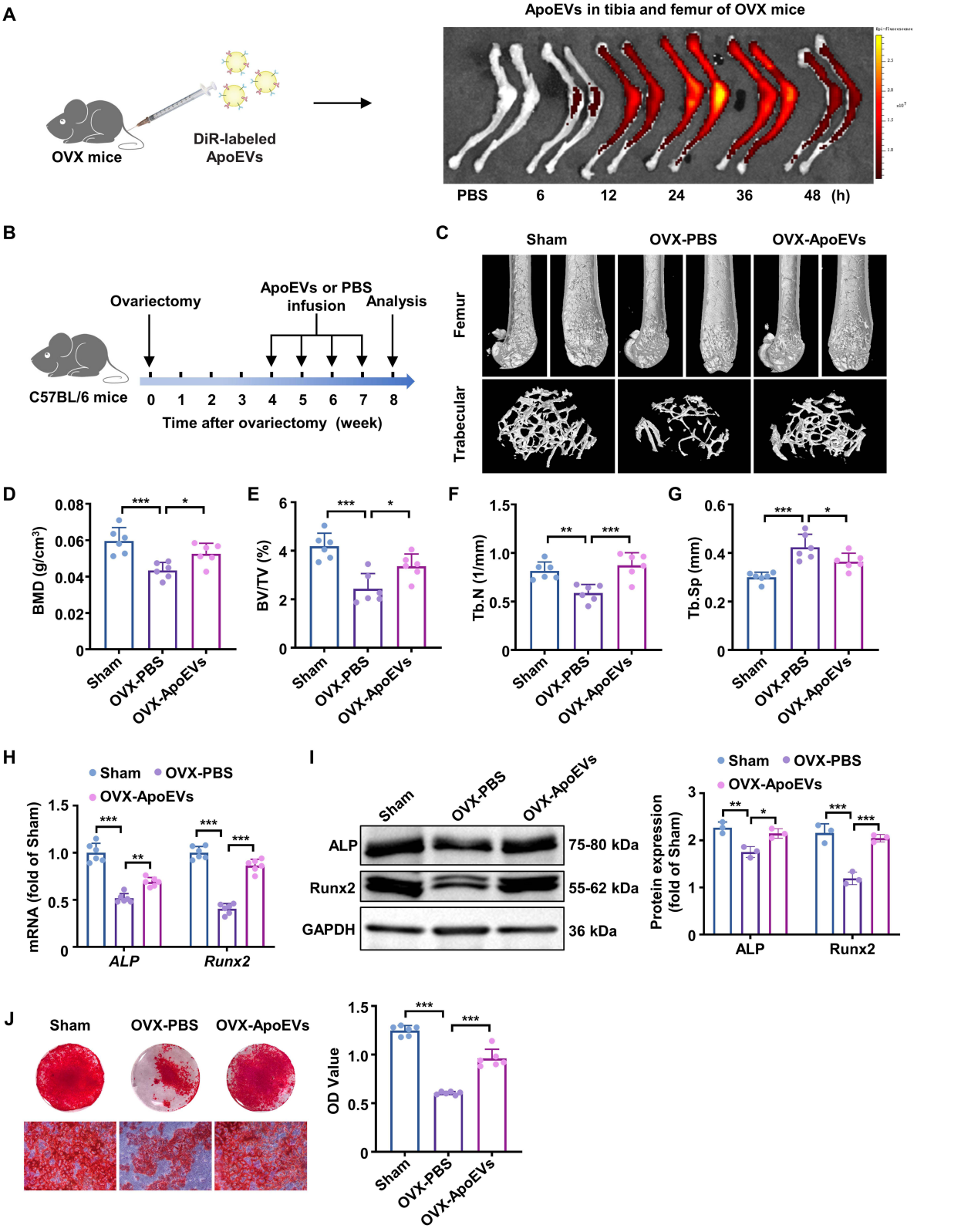

Figure 2 Systemic infusion of T cell-derived ApoEVs ameliorates osteopenia in OVX mice. (**A**). Schematic diagram showing injection and in vivo tracking of DiR-labeled ApoEVs (left). Representative fluorescence images of tibiae and femurs 6, 12, 24, 36 and 48 h after intravenous injection of DiR-labeled ApoEVs in OVX mice (right). (**B**) Schematic diagram indicating the study design for the treatment of osteoporosis mice. (**C**) Micro-CT analyses of trabecular bone mass in the femurs. (**D-G**) Quantitative analyses of BMD (**D**), BV/TV (**E**), Tb. N (**F**) and Tb. Sp (**G**) (N = 6). (**H**) BMMSCs from each group were isolated and cultured in osteogenic medium. Real-time PCR was performed to detect mRNA expression of *ALP* and *Runx2* on day 5 after osteogenic induction. (**I**) Western blot analysis and quantification of the osteogenic-related proteins ALP and Runx2 on day 10 after osteogenic induction. (**J**) Alizarin red staining and quantification of mineralized nodules were performed on day 21 after induction. Data are presented as mean ± SD; *P< 0.05; **P< 0.01; ***P< 0.001 by one-way ANOVA with Tukey's post hoc test.

https://doi.org/10.2147/IJN.S491222

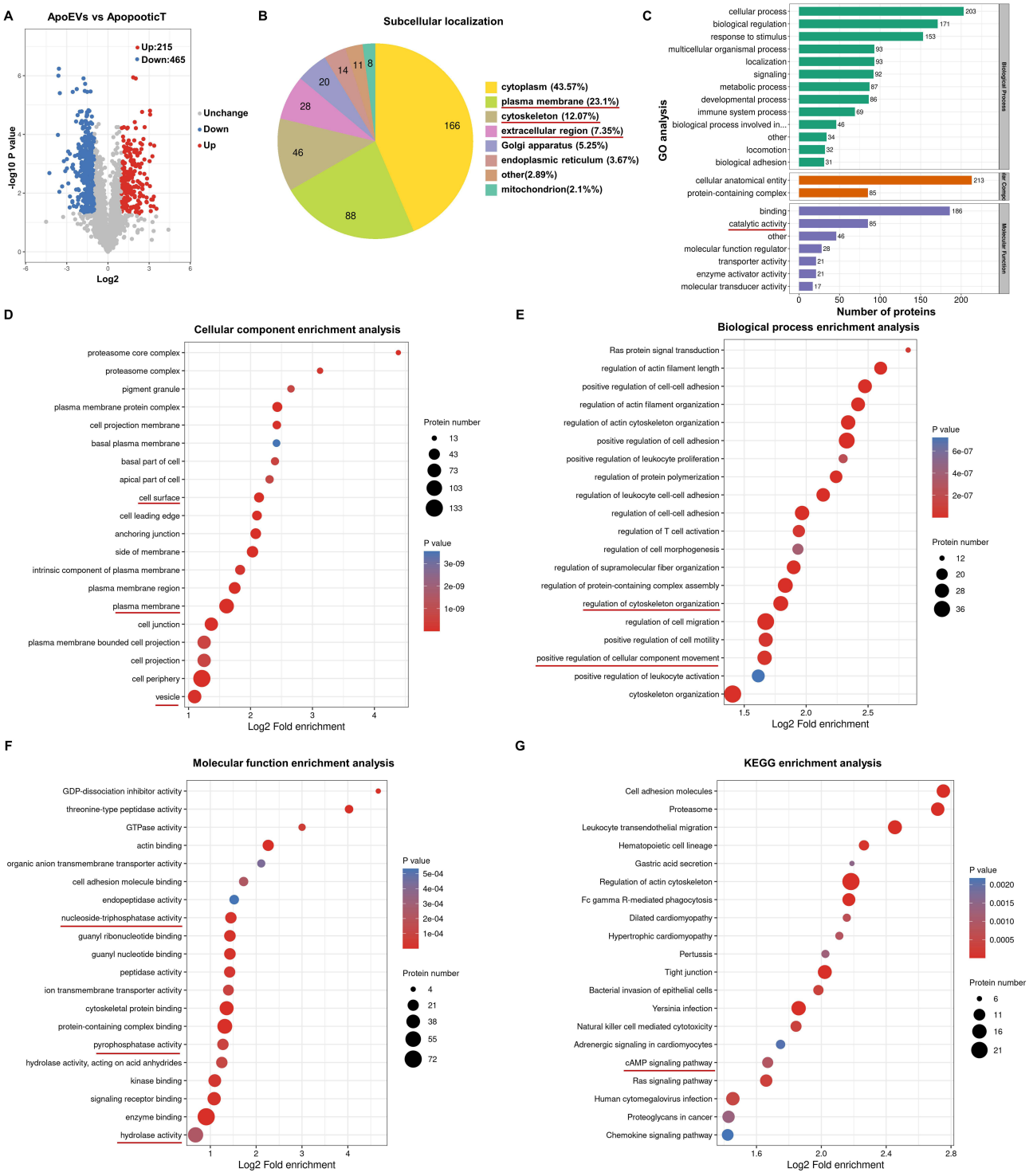

Figure 3 T cell-derived ApoEVs are enriched with specific ectonucleotidases. (**A**). Volcano plot showing significantly upregulated (red dots) and downregulated (blue dots) proteins in ApoEVs compared with apoptotic T cells (ApoEVs-free). (**B**) Subcellular localization of significantly upregulated proteins in ApoEVs compared with apoptotic T cells. (**C**) Gene ontology (GO) analysis of significantly upregulated proteins in ApoEVs, categorized into "Biological process", "Cellular component", and "Molecular function". (**D-F**) Cellular component (**D**), biological process (**E**), and molecular function enrichment (**F**) analyses of significantly upregulated proteins in ApoEVs. The Y-axis represents GO terms and the X-axis represents rich factor. The color of the bubble represents enrichment significance and the size of the bubble represents number of upregulated proteins. (**G**) Kyoto Encyclopedia of Genes and Genomes (KEGG) pathway enrichment analysis of significantly upregulated proteins in ApoEVs. The Y-axis represents KEGG pathways and the X-axis represents rich factor. The color of the bubble represents enrichment significance and the size of the bubble represents number of upregulated proteins.

G). The elucidation of the subcellular localization of proteins is of great importance for further understanding the function of proteins. Subcellular localization prediction revealed that most of the upregulated proteins were localized in the cytoplasm (43.57%), followed by plasma membrane (23.1%), cytoskeleton (12.07%) and extracellular region (7.35%) (Figure 3B). As to the functional annotations based on the GO database, the upregulated proteins were included into multiple terms within the three categories: biological process, cellular component, and molecular function (Figure 3C). GO analysis suggesting that the proteins loaded on ApoEVs perform various biological functions, including "catalytic activity" (Figure 3C). Cellular component enrichment analysis revealed that ApoEVs exhibited increased expression of proteins located on cell surface, plasma membrane, and vesicles (Figure 3D). Biological process enrichment revealed that ApoEVs had increased expression of proteins with regulatory functions, including "regulation of cytoskeleton organization" and "positive regulation of cellular component movement" (Figure 3E). Molecular function enrichment analysis demonstrated elevated expression of proteins with catalytic activities including "nucleoside triphosphatase activity", "pyrophosphatase activity", and "hydrolase activity" in ApoEVs (Figure 3F). Furthermore, we explored the pathways that were involved in the upregulated proteins via KEGG pathway analysis. Results showed that these proteins were associated with "cAMP signaling pathway" (Figure 3G). These results indicated that ApoEVs are enriched with a group of functional proteins that may possess nucleoside triphosphatase (NTPase) activity, pyrophosphatase activity and are highly likely to be localized on the membrane surface of ApoEVs.

ApoEVs Hydrolyze ATP to Adenosine and Promote Bone Regeneration via Surface CD39 and CD73

The above proteomic analysis suggested that ApoEVs may harbor proteins functioning as extracellular nucleoside triphosphatase and pyrophosphatase. Adenosine triphosphate (ATP) has been reported to serve as a substrate for nucleoside triphosphatase and nucleotide pyrophosphatase.[31] Thus, we hypothesized that ApoEVs could hydrolyze ATP via surface enzymes. We established an in vitro reaction system as formerly reported,[32] and found that ApoEVs could hydrolyze ATP dose-dependently (Figure S4). We proceeded to compared the hydrolysis efficiency of ApoEVs with that of apoptotic T cells (ApoEVs-free). Compared with apoptotic T cells, ApoEVs efficiently hydrolyzed ATP, since no to low residual ATP could be detected in the presence of ApoEVs (Figure 4A). Furthermore, we investigated whether there were alterations in extracellular ATP levels in the bone marrow of OVX mice. We found that the extracellular ATP levels in the bone marrow of OVX mice were significantly higher than those in the Sham group (Figure 4B). CD39 (ectonucleoside triphosphate diphosphohydrolase-1) and CD73 (ecto-5′-nucleotidase) are membrane-bound ectonucleotidases known to regulate extracellular ATP and adenosine by hydrolyzing extracellular ATP to adenosine monophosphate (AMP) and AMP to adenosine, respectively.[33] We detected the changes of CD39 and CD73, and found there was a decrease in the expression of both CD39 and CD73 in OVX mice, which was consistent with a reduction in adenosine levels in the OVX group compared to Sham mice (Figure 4C and D). Based on the proteomic analysis which suggesting the potential role of ApoEVs as extracellular nucleoside triphosphatases, we revealed the presence of ectonucleotidases CD39 and CD73 on ApoEVs and found them to be enriched on ApoEVs (Figure 4E). Further characterization of CD39 and CD73 localization was conducted by immunoelectron microscopy, affirming their presence on the membrane surface of ApoEVs (Figure 4F). We proceeded to assess the enzymatic activity of CD39 and CD73 on the surface of ApoEVs in vitro. The results suggested that ApoEVs hydrolyze ATP dose-dependently, which can be significantly mitigated by POM-1 (POM, a CD39 inhibitor) (Figure 4G). Similarly, the levels of adenosine, the hydrolysis products of ATP, increased dose-dependently and could be significantly attenuated by POM or PSB-12379 (PSB, a CD73 inhibitor) (Figure 4H). These results collectively indicated that CD39 and CD73 are enriched on the membrane surface of ApoEVs, and ApoEVs hydrolyze extracellular ATP to adenosine through its surface-bound CD39 and CD73 in vitro.

Moreover, to investigate whether ApoEVs can hydrolyze ATP via surface CD39 and CD73 in vivo, OVX mice were intravenously infused with PBS, ApoEVs, POM- or PSB-pretreated ApoEVs, respectively (Figure 5). Compared with the PBS control group, mice injected with ApoEVs showed a reduction in extracellular ATP levels in bone marrow, which was counteracted when ApoEVs were pre-incubated with POM (ApoEVs+POM) (Figure 5A). Additionally, the application of PSB did not affect the efficacy of ApoEVs in ATP hydrolysis (Figure 5A). Correspondingly, the levels of adenosine in each group of animals changed, with ApoEVs infusion increasing adenosine concentration compared to the PBS group, while

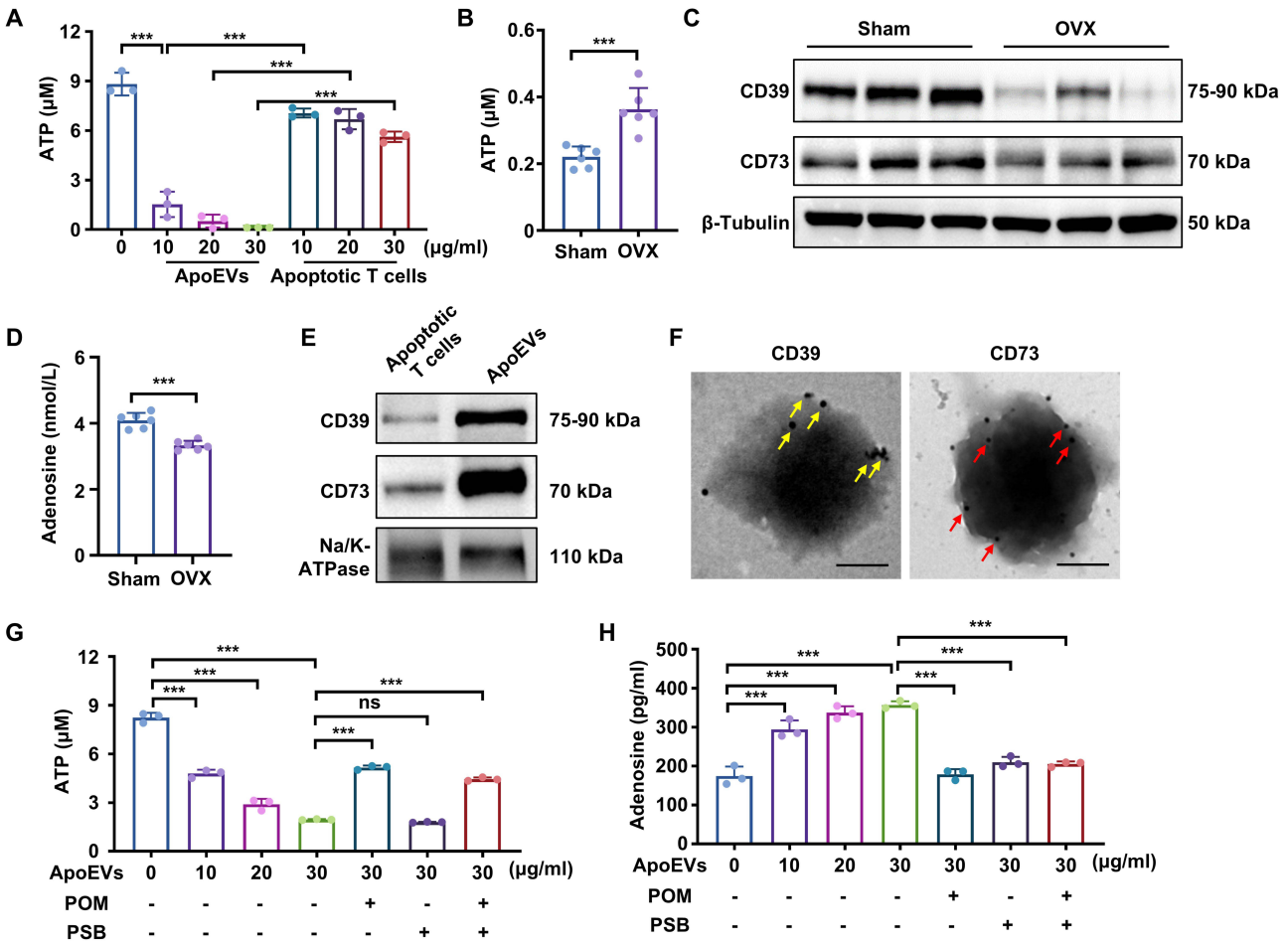

Figure 4 ApoEVs hydrolyze ATP to adenosine via surface CD39 and CD73. (**A**) The activity of ApoEVs and apoptotic T cells to hydrolyze ATP was measured in vitro (N = 3). (**B**) Extracellular ATP concentration in bone marrow plasma of sham and OVX animals (N = 6). (**C**) Western blot analysis of CD39 and CD73 in bone marrow of sham and OVX animals. (**D**) Extracellular adenosine concentration in bone marrow plasma of sham and OVX animals. (**E**) Western blot analysis of CD39 and CD73 on the membrane of apoptotic T cells and ApoEVs. (**F**) Immunoelectron microscopy detection of CD39 and CD73 on ApoEVs (scale bar = 200 nm). Yellow arrows indicate CD39 and red arrows indicate CD73 adhered by gold particles. (**G**) The activity of ApoEVs to hydrolyze ATP with or without POM (a CD39 inhibitor) or PSB (a CD73 inhibitor) was determined in vitro (N = 3). (**H**) The activity of ApoEVs in hydrolyzing ATP to adenosine with or without POM or PSB was determined in vitro (N = 3). Data are presented as mean ± SD; ns, not significant; ***P< 0.001 by one-way ANOVA with Tukey's post hoc test or unpaired Student's *t* test.

POM or PSB pre-treated ApoEVs attenuated this effect (Figure 5B). Based on the above observation, we aimed to elucidate whether ApoEVs promote bone mass recovery by hydrolyzing ATP through surface CD39 and CD73. Micro-CT analysis revealed that the bone mass recovery effect of ApoEVs, as observed in Figure 2C, was reversed by POM or PSB pretreatment (Figure 5C). Consistently, measurements of BMD, BV/TV, Tb. N, and Tb. Sp supported this conclusion (Figure 5D–G). These data indicated that CD39 and CD73 are exposed on the surface of ApoEVs, facilitating the hydrolysis of ATP to adenosine, thereby promoting bone regeneration in OVX mice. Adenosine is a potent anti-inflammatory modulator and is considered a crucial mediator of the immune response.[34,35] The immune microenvironment plays an important role in bone regeneration. We detected the pro-inflammatory cytokines in the serum of OVX mice, and found that IFN-γ (Figure 5H), IL-17 (Figure 5I) and TNF-α (Figure 5J) were all decreased in the ApoEVs group compared with those in the PBS group, while POM or PSB pre-treated ApoEVs attenuated this effect (Figure 5H–J). These results indicated that ApoEVs-generated adenosine inhibits the inflammatory response, thus providing a favorable microenvironment for bone regeneration.

ApoEVs Generated Adenosine Promotes Bone Regeneration via A2BR Signaling

In addition to inhibiting the inflammatory response, studies have implicated the importance of adenosine and its receptors in bone fracture repair and bone homeostasis.[36] The BMMSCs cultured in osteogenic induction medium supplemented

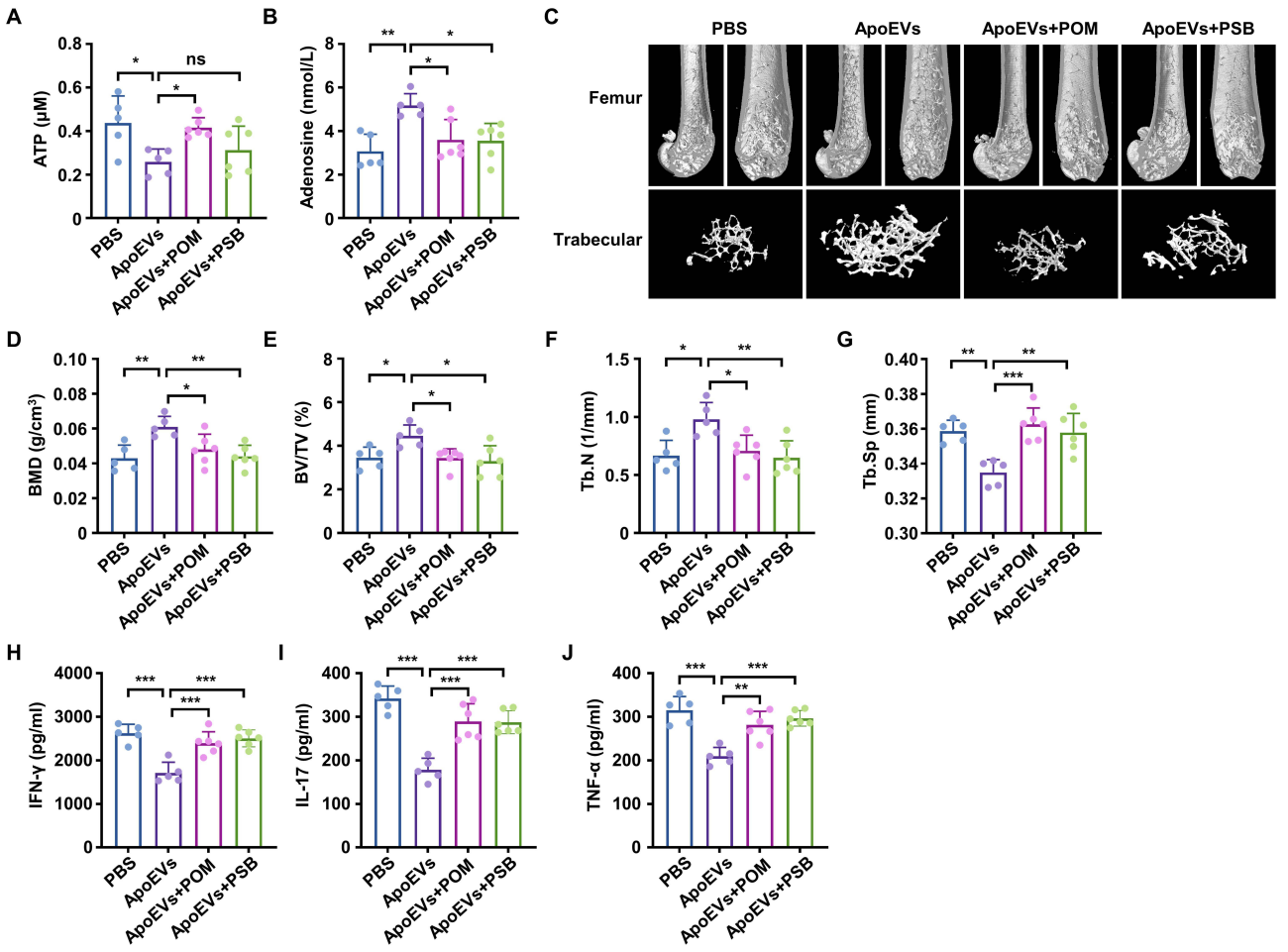

Figure 5 ApoEVs promote bone regeneration via surface CD39 and CD73. OVX mice were divided into four groups and injected with PBS, ApoEVs, and POM or PSB pretreated ApoEVs, respectively (N = 5–6). Extracellular ATP (**A**) and adenosine (**B**) concentration in bone marrow plasma in different groups of mice were detected. (**C**) Micro-CT analyses of trabecular bone mass in the femurs. (**D-G**) Quantitative analyses of BMD (**D**), BV/TV (**E**), Tb. N (**F**) and Tb. Sp (**G**). (**H-J**) ELISA assays of IFN-γ (**H**), IL-17 (**I**) and TNF-α (**J**) concentrations in the serum of peripheral blood from indicated groups. Data are presented as mean ± SD; ns, not significant; *P< 0.05; **P< 0.01; ***P< 0.001 by one-way ANOVA with Tukey's post hoc test.

with adenosine showed an up regulation of A2BR expression with no considerable differences in the expression of other adenosine receptors, such as A1R, A2AR, or A3R (Figure 6A). In the present study, to verify whether ApoEVs-generated adenosine promotes bone mass recovery by A2BR signaling, OVX mice were treated with ApoEVs in the presence or absence of a potent and selective A2BR antagonist BAY-545 (BAY), with PBS-treated mice serving as controls. Micro-CT scanning revealed a significant reduction in bone loss in OVX mice treated with ApoEVs compared with those in the PBS group (Figure 6B). However, this beneficial effect of ApoEVs was mitigated when mice were pre-administered with BAY before receiving ApoEVs (ApoEVs+BAY) (Figure 6B). The quantifications of BMD, BV/TV, Tb. N, and Tb. Sp also support these results (Figure 6C–F). Similarly, we isolated BMMSCs from PBS, ApoEVs, ApoEVs+BAY or BAY-treated OVX mice, and cultured them in osteogenic differentiation medium. The expression of ALP and Runx2 in BMMSCs isolated form ApoEVs-treated OVX mice remarkably increased compared with that in the PBS group (Figure 6G). Moreover, alizarin red staining revealed stronger osteoblast activity in the ApoEVs group than that in the PBS group (Figure 6H). In contrast, no significant improvement in osteogenic differentiation was observed in BMMSCs from OVX mice that received ApoEVs+BAY or BAY therapy (Figure 6G and H). These in vivo experimental evidences suggested that ApoEVs treatment inhibits bone loss and rescues the osteogenic deficiency of BMMSCs via A2BR signaling.

https://doi.org/10.2147/IJN.S491222

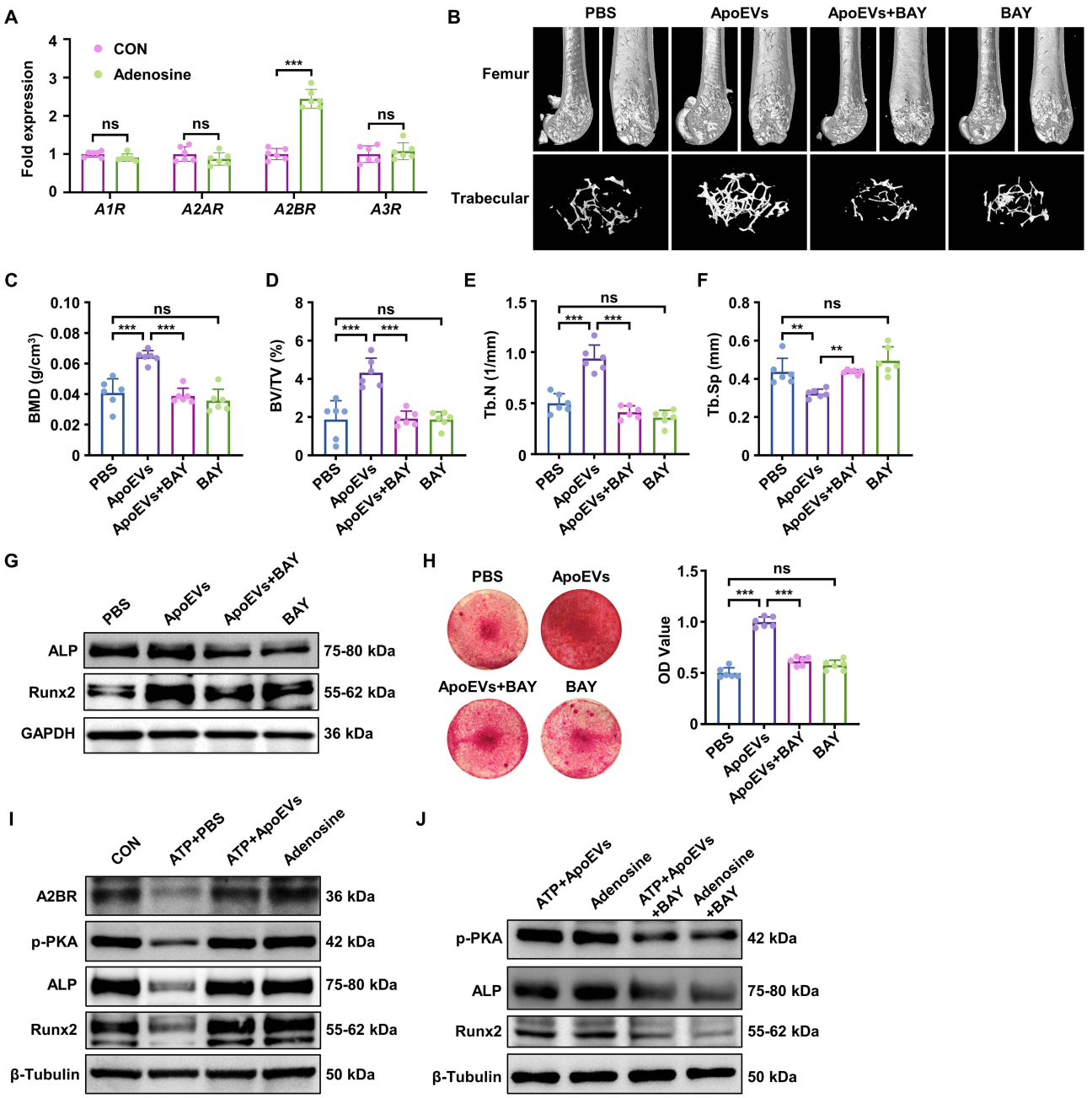

Figure 6 ApoEVs generated adenosine promotes bone regeneration via A2B receptor (A2BR) signaling. (**A**) BMMSCs isolated from C57BL/6 mice were cultured in osteogenic induction medium (CON) or adenosine-supplemented osteogenic induction medium (Adenosine). Real-time PCR was performed to detect mRNA expression of *A1R*, *A2AR*, *A2BR* and *A3R* on day 14 after osteogenic induction. (**B-F**) OVX mice were divided into four groups and injected with PBS, ApoEVs, ApoEVs+BAY (adenosine receptor antagonist) or BAY, respectively (N = 6). (**B**) Micro-CT analyses of trabecular bone mass in the femurs. (**C-F**) Quantitative analyses of BMD (**C**), BV/TV (**D**), Tb. N (**E**) and Tb. Sp (**F**). (**G**) BMMSCs from each group in (**B**) were isolated and cultured in osteogenic medium. Western blot analysis of the osteogenic-related proteins ALP and Runx2 were conducted on day 10 after osteogenic induction. (**H**) Alizarin red staining and quantification of mineralized nodules were performed on day 21 after induction. (**I**) BMMSCs isolated form C57BL/6 mice were cultured for osteogenic induction (CON group). ATP was supplemented to simulate the elevated extracellular ATP levels observed in OVX mice. Subsequently, PBS or ApoEVs were introduced into the medium (ATP+PBS or ATP+ApoEVs groups). The osteogenic medium supplemented with adenosine served as the positive control (Adenosine group). Western blot results shown the expression of A2BR, p-PKA, ALP and Runx2. (**J**) A2BR was blocked with a selective A2BR antagonist, BAY. Western blot results shown the expression of p-PKA, ALP and Runx2. Data are presented as mean ± SD; ns, not significant; **P< 0.01; ***P< 0.001 by one-way ANOVA with Tukey's post hoc test.

To further explore the downstream molecular mechanism of ApoEVs-generated adenosine in promoting osteogenesis in vitro, BMMSCs were isolated form C57BL/6 mice and cultured for osteogenic induction (CON group). ATP was supplemented into the osteogenic medium to simulate the elevated extracellular ATP levels observed in OVX mice.

Subsequently, PBS or ApoEVs were introduced into the medium (ATP+PBS or ATP+ApoEVs groups). The osteogenic medium supplemented with adenosine served as the positive control (Adenosine group). Compare with the control group, it was observed that ATP suppressed the expression of A2BR, while the introduction of ApoEVs resulted in a recovery of A2BR expression (Figure 6I). Similar results were observed in the phosphorylation of protein kinase A (p-PKA), downstream of A2BR signaling. In addition, the osteogenic markers ALP and Runx2 were inhibited by ATP, whereas treatment with ApoEVs restored their expression (Figure 6I). These results are not surprising, as ApoEVs could hydrolyze ATP to adenosine, which subsequently activates A2BR and induces PKA phosphorylation, thereby promoting the osteogenesis of BMMSCs. To further validate that ApoEVs-generated adenosine promotes osteogenesis via A2BR and downstream PKA, we blocked A2BR with a selective A2BR antagonist, BAY, as stated above, and assessed the phosphorylation of PKA along with the osteogenic markers ALP and Runx2 (Figure 6J). As expected, BMMSCs in the ATP+ApoEVs group exhibited comparable levels of p-PKA, ALP, and Runx2 expression to those treated with adenosine (Figure 6J). By contrast, when these cells were treated with BAY in combination, both the phosphorylation of PKA and expression of ALP and Runx2 decreased (Figure 6J). These in vitro experimental findings further substantiate that ApoEVs-generated adenosine promotes osteogenesis through A2BR and downstream PKA signaling.

Discussion

Osteoporosis is a major chronic disease worldwide in postmenopausal women and aging population and frequently leads to fragility fractures, which bring about low quality of life, increased mortality and high healthcare costs.[1] The most regular drugs for osteoporosis are denosumab and bisphosphonates, which inhibit the resorption of bone. However, these treatments may impair intrinsic repair mechanisms and increase the risk of atypical femur fractures.[2,3] Thus, it is required to develop more ideal strategy for the prevention and treatment of osteoporosis. With the advancement of regenerative medicine, ApoEVs generated by different apoptotic cells have emerged as a promising therapeutic option for tissue regeneration due to their low immunogenicity and high biological compatibility.[11–13,15] In this study, we demonstrated that T cell-derived ApoEVs ameliorates osteopenia, the most important finding was that ApoEVs are enriched with CD39 and CD73 on their membrane surface, enabling them to hydrolyze extracellular ATP to adenosine. ApoEVs generated adenosine regulates the immune microenvironment and promotes bone regeneration via A2BR signaling. These findings provide a new insight into the understanding of ApoEVs and reference for future studies.

Apoptosis is a tightly regulated cell death process, there is now increasing evidence to suggest that ApoEVs released from cells during apoptosis is closely related to tissue homeostasis.[13,17,29,37] It has been reported that donor MSCs release ApoEVs to activate autophagy in recipient cells, thereby promoting angiogenesis to improve myocardial infarction or enhance dental pulp regeneration.[14,15] As for the study of ApoEVs in promoting bone regeneration, our results are in line with previous studies which shown that circulating ApoEVs maintain mesenchymal stem cell homeostasis and ameliorate osteopenia via transferring multiple cellular factors.[29] To achieve satisfactory bone targeting capacity of natural ApoEVs, researchers also engineered ApoEVs with bone-targeting functions which could significantly promote osteogenesis and alleviate osteoporosis compared with natural ApoEVs.[38]

It has been established that lymphocytes apoptosis and ApoEVs derived from lymphocytes play a crucial role in regulating inflammation and maintaining physiological homeostasis.[10,17] ApoEVs released by T cells could target the intestines of abdominal irradiated mice and alleviate radiation enteritis.[17] Moreover, engineered chimeric T cell-derived ApoEVs, functionalized with natural membrane and modular delivery system, can effectively modulate inflammation and ameliorate the inflammatory bowel diseases.[18] These advancements highlight the substantial potential of T cell-derived ApoEVs for various biomedical applications. Based on our previous study, we reported that inducing apoptosis in activated T cell in vivo restores immune homeostasis and promotes bone mass recovery in osteoporotic mice.[10] As a continuation of the above studies, we isolated ApoEVs and apoptotic T cells (ApoEVs-free). We found that ApoEVs, but not apoptotic T cells, ameliorate osteopenia and rescues the osteogenic deficiency of BMMSCs in OVX mice. This is not contradictory to our previous results since the apoptosis of T cells in vivo would subsequently produce ApoEVs to further exert biological functions. The present study emphasizes the necessity and importance of the generation of ApoEVs during cell apoptosis.

While extracellular vesicle (EVs) have been recognized as carriers of genetic information, additional unique advantages that they could provide for cellular communication remain unclear. Given their small size, EVs have a large surface compared to volume and provide substantial membrane surface area for long-distance cellular communication.[19] A recent study provided evidence to support that EVs confer a benefit or survival advantage to their parental cells by serving as decoys to trap and neutralize bacterial toxins.[39] This study suggests that EVs can exert their biological functions by specific membrane receptor binding capacity. Similarly, researchers found that transferrin receptors (TfR), are integrated on the EVs surface, which ensures the iron recycling capacity of EVs through capture of the iron-containing molecules to facilitate iron recycling.[40] These studies suggest a shift in perspective from viewing EVs merely as transporters of relevant nucleic acids and proteins to considering their unique biophysical properties as presentation platforms for long-distance, contact-dependent signaling.

CD39 and CD73 are membrane-bound ectonucleotidases, EVs enriched with CD39 and CD73 are immune suppressive.[41] It has been reported that exosomes derived from diverse cancer cells express CD39 and CD73, which suppress T cells through adenosine production.[42] As to T cell-derived EVs, the enrichment of CD73 on EVs derived from CD8 T cells hydrolyzes AMP and promotes the production of adenosine, which plays an immunosuppressive role.[43] Here, we confirmed that T cell-derived ApoEVs are enriched with CD39 and CD73, enabling them to hydrolyze extracellular ATP to adenosine, and promote bone regeneration via A2BR and PKA signaling pathway. Although in this study we have focused on CD39 and CD73 on the surface membrane of ApoEVs, other ectonucleotidases and molecules influencing extracellular ATP and adenosine were not investigated. Furthermore, while other studies have monitored bone mass over a longer duration post-discontinuation of extracellular vesicle administration, our observation period was relatively short. Consequently, there is a pressing need for further research to investigate the long-term efficacy of ApoEVs treatment. Such research will not only provide a robust theoretical foundation but also crucial experimental support for the future clinical translation of ApoEVs.

Conclusions

In summary, our findings revealed that T cell-derived ApoEVs are enriched with CD39 and CD73 on their membrane surface, enabling them to hydrolyze extracellular ATP to adenosine. The adenosine generated by ApoEVs regulates the immune microenvironment and facilitated osteogenic differentiation by activating the A2BR and downstream PKA signaling pathway. Our study extends the understanding of EVs, from viewing EVs merely as transporters to considering their unique biophysical properties, thus providing new ideas for the EVs-based therapy in tissue regeneration and immune disorders.

Funding

This work was supported by the National Natural Science Foundation of China (82202341, 82301099, 82170925, 82000841, and 82201133), China Postdoctoral Science Foundation (2022M721529), 2024 Guangzhou Special Topic on Fundamental and Applied Basic Research (Science and Technology Elite “Pioneering” Project) (SL2023A04J02637), the Shenzhen Science and Technology Program (JCYJ20210324105813036), Shenzhen High-level Hospital Construction Fund, Peking University Shenzhen Hospital Scientific Research Fund (KYQD2023252), Young Physicians Cultivation Program of Xijing Hospital (XJZT24QN06), and Science Research Cultivation Program of Stomatological Hospital, Southern Medical University (PY2021010).

Disclosure

The authors declare no competing interests in this work.

References

1. Black DM, Rosen CJ. Clinical Practice. Postmenopausal Osteoporosis. *New Engl J Med*. 2016;374(3):254–262. doi:10.1056/NEJMcp1513724
2. Song S, Guo Y, Yang Y, Fu D. Advances in pathogenesis and therapeutic strategies for osteoporosis. *Pharmacol Ther*. 2022;237:108168. doi:10.1016/j.pharmthera.2022.108168

3. Khosla S, Hofbauer LC. Osteoporosis treatment: recent developments and ongoing challenges. *Lancet Diabetes Endocrinol*. 2017;5(11):898–907. doi:10.1016/S2213-8587(17)30188-2
4. Gehrke B, Alves Coelho MC, Brasil d'Alva C, Madeira M. Long-term consequences of osteoporosis therapy with bisphosphonates. *Arch Endocrinol Metab*. 2023;68:e220334. doi:10.20945/2359-4292-2022-0334
5. Rossouw JE, Anderson GL, Prentice RL, et al. Risks and benefits of estrogen plus progestin in healthy postmenopausal women: principal results From the Women's Health Initiative randomized controlled trial. *JAMA*. 2002;288(3):321–333. doi:10.1001/jama.288.3.321
6. Zhang W, Dang K, Huai Y, Qian A. Osteoimmunology: the regulatory roles of T lymphocytes in osteoporosis. *Front Endocrinol*. 2020;11:465. doi:10.3389/fendo.2020.00465
7. Cenci S, Weitzmann MN, Roggia C, et al. Estrogen deficiency induces bone loss by enhancing T-cell production of TNF-alpha. *J Clin Invest*. 2000;106(10):1229–1237. doi:10.1172/JCI11066
8. Medina CB, Mehrotra P, Arandjelovic S, et al. Metabolites released from apoptotic cells act as tissue messengers. *Nature*. 2020;580 (7801):130–135. doi:10.1038/s41586-020-2121-3
9. Cao C, Yu M, Chai Y. Pathological alteration and therapeutic implications of sepsis-induced immune cell apoptosis. *Cell Death Dis*. 2019;10 (10):782. doi:10.1038/s41419-019-2015-1
10. Yang X, Zhou F, Yuan P, et al. T cell-depleting nanoparticles ameliorate bone loss by reducing activated T cells and regulating the Treg/Th17 balance. *Bioact Mater*. 2021;6(10):3150–3163. doi:10.1016/j.bioactmat.2021.02.034
11. Zheng C, Sui B, Zhang X, et al. Apoptotic vesicles restore liver macrophage homeostasis to counteract type 2 diabetes. *J Extracell Vesicles*. 2021;10(7):e12109. doi:10.1002/jev2.12109
12. Li M, Liao L, Tian W. Extracellular vesicles derived from apoptotic cells: an essential link between death and regeneration. *Front Cell Develop Biol*. 2020;8:573511. doi:10.3389/fcell.2020.573511
13. Zhu Y, Chen X, Liao Y. Mesenchymal stem cells-derived apoptotic extracellular vesicles (ApoEVs): mechanism and application in tissue regeneration. *Stem Cells*. 2023;41(9):837–849. doi:10.1093/stmcls/sxad046
14. Liu H, Liu S, Qiu X, et al. Donor MSCs release apoptotic bodies to improve myocardial infarction via autophagy regulation in recipient cells. *Autophagy*. 2020;16(12):2140–2155. doi:10.1080/15548627.2020.1717128
15. Li Z, Wu M, Liu S, et al. Apoptotic vesicles activate autophagy in recipient cells to induce angiogenesis and dental pulp regeneration. *Mol Ther*. 2022;30(10):3193–3208. doi:10.1016/j.ymthe.2022.05.006
16. Ma L, Chen C, Liu D, et al. Apoptotic extracellular vesicles are metabolized regulators nurturing the skin and hair. *Bioact Mater*. 2023;19:626–641. doi:10.1016/j.bioactmat.2022.04.022
17. Zhou Y, Bao L, Gong S, et al. T cell-derived apoptotic extracellular vesicles hydrolyze cGAMP to alleviate radiation enteritis via surface enzyme ENPP1. *Adv Sci*. 2024;11(31):e2401634. doi:10.1002/advs.202401634
18. Dou G, Tian R, Liu X, et al. Chimeric apoptotic bodies functionalized with natural membrane and modular delivery system for inflammation modulation. *Sci Adv*. 2020;6(30):eaba2987. doi:10.1126/sciadv.aba2987
19. Buzas EI, Toth EA, Sodar BW, Szabo-Taylor KE. Molecular interactions at the surface of extracellular vesicles. *Semin Immunopathol*. 2018;40 (5):453–464. doi:10.1007/s00281-018-0682-0
20. Jahnke K, Staufer O. Membranes on the move: the functional role of the extracellular vesicle membrane for contact-dependent cellular signalling. *J Extracell Vesicles*. 2024;13(4):e12436. doi:10.1002/jev2.12436
21. Allard B, Longhi MS, Robson SC, Stagg J. The ectonucleotidases CD39 and CD73: novel checkpoint inhibitor targets. *Immunol Rev*. 2017;276 (1):121–144. doi:10.1111/imr.12528
22. Antonioli L, Pacher P, Vizi ES, Haskó G. CD39 and CD73 in immunity and inflammation. *Trends Mol Med*. 2013;19(6):355–367. doi:10.1016/j.molmed.2013.03.005
23. de Andrade Mello P, Coutinho-Silva R, Savio LEB. Multifaceted effects of extracellular adenosine triphosphate and adenosine in the tumor-host interaction and therapeutic perspectives. *Front Immunol*. 2017;8:1526. doi:10.3389/fimmu.2017.01526
24. Kvist TM, Schwarz P, Jorgensen NR. The P2X7 receptor: a key player in immune-mediated bone loss? *Sci World J*. 2014;2014:954530. doi:10.1155/2014/954530
25. Katebi M, Soleimani M, Cronstein BN. Adenosine A2A receptors play an active role in mouse bone marrow-derived mesenchymal stem cell development. *J Leukoc Biol*. 2009;85(3):438–444. doi:10.1189/jlb.0908520
26. Fatokun AA, Stone TW, Smith RA. Hydrogen peroxide-induced oxidative stress in MC3T3-E1 cells: the effects of glutamate and protection by purines. *Bone*. 2006;39(3):542–551. doi:10.1016/j.bone.2006.02.062
27. Sui B, Wang R, Chen C, et al. Apoptotic vesicular metabolism contributes to organelle assembly and safeguards liver homeostasis and regeneration. *Gastroenterology*. 2024;167(2):343–356. doi:10.1053/j.gastro.2024.02.001
28. Lu J, Sun M, Zhang J, et al. Benidipine-loaded nanoflower-like magnesium silicate improves bone regeneration. *Bio-Des Manuf*. 2023;6 (5):507–521. doi:10.1007/s42242-023-00240-8
29. Liu D, Kou X, Chen C, et al. Circulating apoptotic bodies maintain mesenchymal stem cell homeostasis and ameliorate osteopenia via transferring multiple cellular factors. *Cell Res*. 2018;28(9):918–933. doi:10.1038/s41422-018-0070-2
30. Bussolati B, Camussi G. Renal injury: early apoptotic extracellular vesicles in injury and repair. *Nat Rev Nephrol*. 2017;13(9):523–524. doi:10.1038/nrneph.2017.117
31. Longhi MS, Feng L, Robson SC. Targeting ectonucleotidases to treat inflammation and halt cancer development in the gut. *Biochem Pharmacol*. 2021;187:114417. doi:10.1016/j.bcp.2021.114417
32. Perrot I, Michaud HA, Giraudon-Paoli M, et al. Blocking antibodies targeting the CD39/CD73 immunosuppressive pathway unleash immune responses in combination cancer therapies. *Cell Rep*. 2019;27(8):2411–25e9. doi:10.1016/j.celrep.2019.04.091
33. Yegutkin GG. Enzymes involved in metabolism of extracellular nucleotides and nucleosides: functional implications and measurement of activities. *Crit Rev Biochem Mol Biol*. 2014;49(6):473–497. doi:10.3109/10409238.2014.953627
34. Hasko G, Cronstein B. Regulation of inflammation by adenosine. *Front Immunol*. 2013;4:85. doi:10.3389/fimmu.2013.00085
35. Pasquini S, Contri C, Borea PA, Vincenzi F, Varani K. Adenosine and inflammation: here, there and everywhere. *Int J mol Sci*. 2021;22(14):7685. doi:10.3390/ijms22147685

36. Ham J, Evans BA. An emerging role for adenosine and its receptors in bone homeostasis. *Front Endocrinol*. 2012;3:113. doi:10.3389/fendo.2012.00113
37. Yu L, Dou G, Kuang H, et al. Apoptotic extracellular vesicles induced endothelial cell-mediated autologous stem cell recruitment dominates allogeneic stem cell therapeutic mechanism for bone repair. *ACS Nano*. 2024;18(12):8718–8732. doi:10.1021/acsnano.3c11050
38. Gui L, Ye Q, Yu L, et al. Bone-targeting peptide and RNF146 modified apoptotic extracellular vesicles alleviate osteoporosis. *Int J Nanomed*. 2024;19:471–488. doi:10.2147/IJN.S433511
39. Keller MD, Ching KL, Liang FX, et al. Decoy exosomes provide protection against bacterial toxins. *Nature*. 2020;579(7798):260–264. doi:10.1038/s41586-020-2066-6
40. Kuang H, Dou G, Cheng L, et al. Humoral regulation of iron metabolism by extracellular vesicles drives antibacterial response. *Nat Metab*. 2023;5(1):111–128. doi:10.1038/s42255-022-00723-5
41. Zhang F, Li R, Yang Y, et al. Specific decrease in B-cell-derived extracellular vesicles enhances post-chemotherapeutic CD8(+) T cell responses. *Immunity*. 2019;50(3):738–50e7. doi:10.1016/j.immuni.2019.01.010
42. Clayton A, Al-Taei S, Webber J, Mason MD, Tabi Z. Cancer exosomes express CD39 and CD73, which suppress T cells through adenosine production. *J Immunol*. 2011;187(2):676–683. doi:10.4049/jimmunol.1003884
43. Schneider E, Winzer R, Rissiek A, et al. CD73-mediated adenosine production by CD8 T cell-derived extracellular vesicles constitutes an intrinsic mechanism of immune suppression. *Nat Commun*. 2021;12(1):5911. doi:10.1038/s41467-021-26134-w